

# INTERNATIONAL JOURNAL OF ENGINEERING SCIENCES & MANAGEMENT

## PERFORMANCE EVALUATION OF UWB-IR SYSTEM

**Dheeraj Patil, Pallavi Pahadiya**  
Sagar Institute of Research and Technology, Indore  
[ppahadiya@trubainstitute.ac.in](mailto:ppahadiya@trubainstitute.ac.in)  
[dheerajpatil039@gmail.com](mailto:dheerajpatil039@gmail.com)

### ABSTRACT

Ultra Wideband Technology for commercial communication application is a recent innovation. The short range wireless systems have recently gained a lot of attention to provide multimedia communication and to run high speed applications around a user centric concept in so called Wireless Personal Area Network (WPAN). UWB technology presents itself as a good candidate for the physical layer of WPAN. In this thesis, a comparative performance analysis of the direct-sequence spread spectrum (DS-SS) for Pulse Position Modulation (PPM) and Pulse Amplitude Modulation (PAM) schemes carried out. The simulation results show that the bit error rate (BER) performance of the DS-SS PAM outperforms the DS-SS PPM systems. Further, study is carried out for selection of transmission pulse to meet the FCC specified frequency mask for indoor applications. The work is extended to cover the link budget analysis for UWB systems also.

The present work can be extended in future to cover the realistic channel models for various applications such as sensor networks, WPAN and multipath etc. Channel coding can also be a promising research direction.

**KEYWORD:-** USB, IR,

### INTRODUCTION

Wireless Sensor Networks can be defined as systems composed of several autonomous nodes linked together by a dedicated wireless link [1]. The nodes architecture may include a microprocessor, several sensor and actuator modules and also a radio communication module on a single board. WSNs support a large range of applications: monitoring, local area control, factory and house automation and tactical applications [1-3]. The case study presented in this paper studies a local area protection system. It is a kind of remote detection and identification application, in which sensor nodes are densely scattered in the protected area to detect or sense intrusion events, generated by intruder nodes presence in their vicinity, in order to report it to a base station for analysis. This can be used to reinforce homeland or military troop's security in a tactical application. The intrinsic constraints when setting up such systems are power efficiency, reliability, latency, simplicity, and small size [1-3]. IR-UWB is a good candidate to satisfy the mentioned constraints because of its interesting characteristics which are low radiated power, simple circuitry, localization ability, high multipath resolution and multiuser access capabilities using Time Hopping (TH) [4-5].

The goal of this paper is to analyze and propose an efficient WSN architecture based on IR-UWB and validate it using engineering simulation. As an alternative MACPHY, layer for 802.15.4a based WSN, several IR-UWB MAC-PHY models have been proposed [6-11]. These models can be divided into two categories: the first one insists on the PHY layer characterization [6-8]. The second one integrates this characterization into the network simulator [9-12]. None of them uses the real pulse propagation delay. Instead, they use a uniformly distributed random value to approximate it. This can be tolerated for the first type of models as they aim to provide a Bit Error Rate versus Signal and Interference to Noise Ratio (BER/SINR) depending on the number of active users. However, when modeling at the network simulator, such approximation can be avoided, as the pulse propagation delay and the number of active users is available.

Indeed, the second type of model does not completely meet the WSN simulation requirements as it does not include sensing and sensor channel models. This paper presents an overview of a new developed simulation platform for IR-UWB that takes into account the previous mentioned aspects. It also presents a comprehensive performance evaluation of WSNs that has been conducted using this platform. The performance evaluation compares distributed MAC protocol for IR-UWB to 802.15.4 Uncoordinated Access. The network performance is evaluated using a detection and identification application and also Constant Bit Rate (CBR) traffic. CBR is included for comparison purposes as it is mainly the used model to simulate WSN traffic.

The remainder of this paper will be organized as follows. Section 2 gives an overview of the developed simulation platform. Section 3 presents the performance evaluation scenario and their numerical analysis results analysis and finally Section 4 concludes.

**SIMULATION PLATFORM OVERVIEW**

We developed a WSN simulator based on IR-UWB in our previous work [13]. The platform development is based on a hardware prototype [5]. It mainly focuses on the IR-UWB PHY and MAC layer accuracy modeling. The PHY layer behavior is modeled by taking into account the pulse collision according to the pulse propagation delay. Slotted and UnSlotted MAC protocols for IR-UWB are modeled. A remote detection and identification application is also included.

**Physical Layer Model**

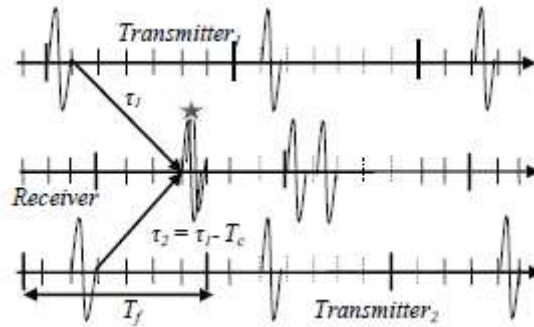


Figure 1: Collision illustration

IR-UWB signals are transmitted in form of very short pulses with low duty cycle (figure 1). The medium is divided into frames and each frame is shared in  $N_h$  chips. The frame and chip duration are  $T_f$  and  $T_c$ , respectively. The transmitted symbol can be repeated following a pseudo random sequence to avoid catastrophic collision under multiuser access conditions [7-8]. Using the Time Hopping Binary Pulse Amplitude Modulation (THBPAM) scheme for example, the  $k$ th user transmitted signal  $s_k(t)$  can be expressed as [7-8]

$$s_k^{(k)}(t) = \sum_{j=-\infty}^{\infty} \sqrt{E_{tx}} x_{tx}(t - jT_f - c_j^k T_c) \quad (1)$$

where  $E_{tx}$  is the transmitted pulse energy;  $x_{tx}$  denotes the basic pulse shape and  $c_j^k$  represents the  $j$ th component of the pseudo random Time Hopping Sequence. The received signal  $r(t)$  when only one user is present can be expressed as

$$r(t) = A S_{tx}(t - \tau) + n(t) \quad (2)$$

$$r(t) = \sum_{j=-\infty}^{\infty} A \sqrt{E_{tx}} x_{tx}(t - jT_f - c_j^k T_c - \tau) + n(t) \quad (3)$$

where  $\tau$  represents the pulse propagation delay and  $n(t)$  is Additive White Gaussian Noise (AWGN) with  $20 N$  power density and  $A$  represents the attenuation the signal experiences during propagation [7-8]. It depends on the considered channel model in terms of path loss, multipath, shadowing. In a multi user scenario where  $N_u$  users are active, the received signal is expressed as

$$r(t) = \sum_{k=1}^{N_u} A_k S_{tx}(t - \tau_k) + n(t) \quad (4)$$

$$r(t) = A_1 S_{tx}(t - \tau_1) + \sum_{k=2}^{N_u} A_k S_{tx}(t - \tau_k) + n(t) \quad (5)$$

where  $\tau_k$  represents the delay associated to the propagation and asynchronism between clocks [7-8].  $A_k$  represents the attenuation of the  $k$ th user's signal ( $k=1$  represents the signal of the user interest). This formulation can be used to characterize the TH-IR-UWB PHY layer in a multi user scenario and directly reports to the network simulator [9-12]; however the used propagation delay does not represent the real propagation delay for the real deployment configuration. The used Bit Error Rate (BER) versus the Signal to Interference and Noise Ratio (SINR) is also based on a perfect power control assumption which is not always realistic.

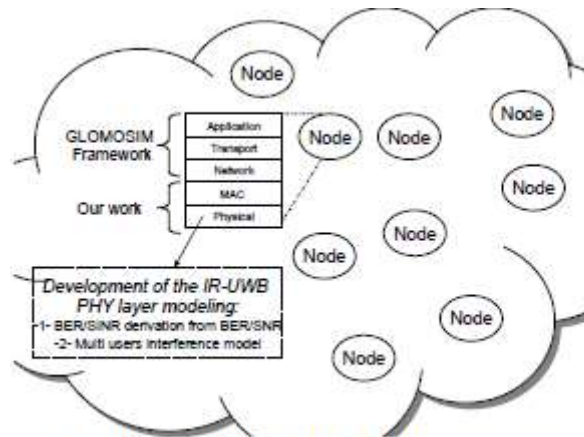


Figure 2: Simulation Methodology Overview

Instead of characterizing BER versus SINR of concurrent transmissions out of the network simulator in a multi user scenario and report it on the network simulator,

our model is based on a two steps characterization process. We first perform an extensive Matlab/Simulink© simulation to obtain the relationship between the BER and the SNR:  $E/N_0$  in a single user scenario. The BER versus SNR for IR-UWB can also be derived from point to point link measurement in the targeted environment.

The multi user interference characterization is reported to the network simulator PHY layer model for more accuracy. This constitutes the second characterization step in our model (figure 2). In this step we model the pulse interference according to the pulses' real propagation delay, during the concurrent transmission, instead of using Gaussian approximation to emulate the multi user interference. Indeed, Gaussian approximation to evaluate multi user interference has been proven to be unrealistic [8]. Moreover, our new scheme avoids an a priori assumption about the propagation delay  $k \tau$ , the number of active users  $N_u$  and the perfect power control ability as they are available during the simulation. The propagation delay is computed according to the node position, the pulse velocity and the occupied bandwidth [13]. The number of active users depends on the number of concurrent transmission being performed. The received power is evaluated according to the used channel model (Free Space, Rice or Rayleigh channel model).

The multiuser access interference is computed and added to the receiver background noise  $n(t)$  on a chip per chip basis. This technique outperforms the model proposed in [9] in terms of accuracy. Indeed, in [9], the pulse propagation delay of concurrent transmission using the same or different THS is mainly modeled at the first characterization stage using a Gaussian approximation [8]. Note that the reception THS at a particular receiver depends on its local view of the medium frame structure (Figure 1). So it may vary depending on the node position and the central frequency of the occupied bandwidth. The  $j$ th component of the reception time hopping sequence of the  $k$ th user at a particular receiver can be expressed as

$$\rho_j^k = (T_c \cdot c_j^k + \tau_k) \bmod T_f \quad (6)$$

The reception THSs are computed and stored in an interference matrix  $M$  (Figure 3). We use an interference vector  $S$  to store the SINR of the signal pulses of the user of interest. For each received pulse, the SINR is dynamically updated. The pulses that interfere with the user of interest (user1) are the reception sequence  $j$ th elements defined by the interfering matrix content such as:

$$(T_c \cdot c_j^1 + \tau_1) \bmod T_f = (T_c \cdot c_j^k + \tau_k) \bmod T_f \quad (7)$$

$$\Leftrightarrow \rho_j^1 = \rho_j^k \quad (8)$$

Doing the parallel between the previous equations and the received power  $k P$  of the concurrent reception, the received signal for the user of interest can be expressed as

$$P_{rx} = P_1 + \sum_{k=2}^{N_k} \left( \bar{P}_k + \frac{N_0}{2} \right) \quad (9)$$

Where  $-k P$  represents the received power of pulses located in the same frame.

$$\bar{P}_k = \begin{cases} P_k, & \text{if } \rho_j^1 = \rho_j^k \\ 0, & \text{otherwise} \end{cases} \quad (10)$$

So the SINR vector S can be obtained as follow where the J<sup>th</sup> component is defined as:

$$S_j = \frac{P_1}{\frac{N_0}{2} + \sum_{k=2}^{N_u} P_k} \quad (11)$$

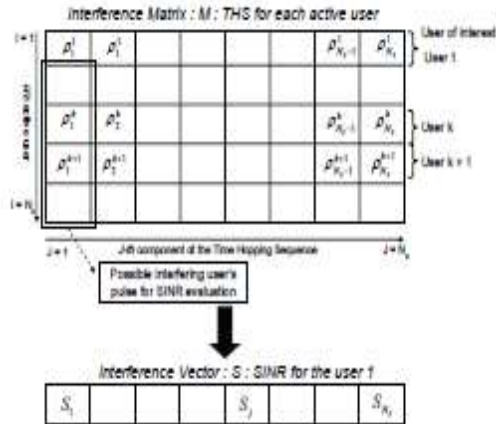


Figure 3: Multi user interference illustration using an interference matrix

This model is based on a single user reception model. However, multi user reception is possible once the preambles are well acquired, which means that the reception THS do not interfere. In this particular case the SINR vector S has to be replaced by an SINR matrix as we are interested in decoding every receiving signal. The presented methodology is generic, thus it can be used for any multiuser access scheme: Frequency Hopping Spread Spectrum (FHSS) as well as Direct Sequence Spread Spectrum (DSSS) for example.

**MAC layer model**

We modeled distributed Medium Access Control protocols for IR-UWB [14]: UnSlotted and Slotted MAC model. These are simple ALOHA [3] [15] like protocols with parameterized reliability and slot size. Their performances are evaluated and presented in the Section 3.

**Sensor and sensing channel model**

Detailed modeling of the sensor device is a key feature to obtain an accurate WSN simulation framework, as it has an impact on the network performance [16-17]. Our model is based on mechanic wave propagation. To set it up, we first characterize the sensor device and sensing channel by considering their important parameters: sampling rate, sensing range, missed detection rate. We use this characterization to mimic the sensor node behavior on the network simulator.

- The sensing range is modeled using a probabilistic detection range instead of full disc coverage.
- The signal propagation is modeled by a two ray ground reflection path loss and a Ricean fading multipath channel model.
- Missed detections are modeled using adjustable parameters.

The principle is summarized as follows: The targeted nodes periodically generate a signal at the sampling rate of the sensor device. This signal is sensed by the sensor node. According to its sensitivity, it detects or not the presence of an intruder.

The two defined thresholds represent the device sensitivity and its detection threshold for correct detection (figure 4). Furthermore, the signal generated by two or more targeted nodes may collide at the sensor device input, thus leading to missed detection. The presence of an intruder or a targeted node may not always be notified by the sensor device because of the additional attenuation due to multipath losses, thus leading to missed detection.

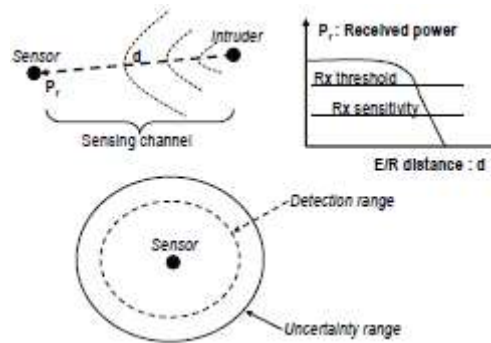


Figure 4: Sensor and sensing channel

This generic method can be used to represent many kind of sensor device behavior, after adjusting the mentioned parameters. An example of a sensor device which can be modeled following the mentioned technique is a binary acoustic sensor present in the Mica Mote hardware. This kind of device provides one bit information regarding the presence or absence of an intruder node in its vicinity without 100% reliability [18].

**USB RADIO LINK AND SIMULATION PARAMETERS**

UWB radio signals must, in principle, coexist with other radio signals. Possible interference from and onto other communications systems must be contained within regulated values that indicate the maximum tolerable power to be present in the air interface at any given frequency, as set by emission masks. In this chapter, we will first analyze how to read and apply an emission mask, and second, we will introduce the methodology for performing a link budget, that is, we will determine the maximum distance of propagation at a given data rate under a maximum probability of error constraint for the UWB point-to-point link.

**Power Limit and Emission Marks**

The power limitation set by emission masks is on the effective radiated power, that is the Effective Isotropic Radiated Power (EIRP) for a given range of operating frequencies, and is given by the product of available power of the transmitter  $P_{TX}$ , which is the maximum power that the transmitter can transfer to the transmitting antenna and the gain of the transmitter antenna  $G_{AT}$ .

$$EIRP = P_{TX} G_{AT} \tag{12}$$

**Link Budget**

The PSD limitation defined by emission masks determines the maximum allowed transmitted power. Given the allowed power, we will now evaluate, under rather simplified hypotheses, the maximum distance over which propagation can occur when a predetermined probability of error must be guaranteed at the receiver, at a given data rate. Decision at the receiver is based on the observation of a received energy  $E$  over a finite time interval, which is composed of mainly two terms: a signal term  $E_r$  and a noise term  $E_{noise}$ . The noise term may include several independent noise sources such as thermal noise, multi-user interference, and so on, that is:

$$E = E_r + \sum_{i=1}^N E_i = E_r + E_{noise} \tag{13}$$

Table 3.1 Simulation Parameters

Specification	Values
Sampling frequency	50e9
Average pulse repetition period	2e-9
Transmitting antenna gain	1
Receiving antenna gain	1
System margin	5 rdB
Order of the derivative	5
Noise figure	7 dB

**THE UWB CHANNEL AND RECEIVER**

This chapter analyzes the signal at the receiver, that is, after propagation over the radio channel, as shown in fig(4.1).

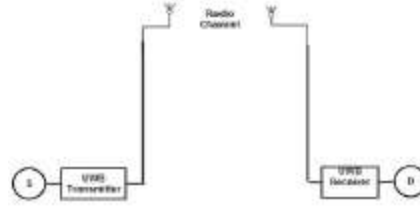


Figure 5: System model for UWB communication

The purpose of this chapter is to investigate how the above models translate in the case of communications systems using IR-UWB. IR-UWB incorporates peculiar features that need to be taken into account for a comprehensive analysis of system design. We first take perfect synchronization between transmitter and receiver, and proceed to give a detailed analysis of receiver structures for different IR-UWB modulation formats, and in particular DS-UWB. The IR-UWB transmitted signal is ideally composed of a sequence of pulses that do not overlap in time. Each pulse is confined within a specific time interval, and the pulse itself has finite duration. While ISI among pulses belonging to the same transmission is ideally absent in the transmitted signal, it might not be so after the signal has traveled through a real channel. Pulses might in fact be delayed by different amounts, and replicas of pulses due to multiple paths might cause ISI. Moreover, in the case of the presence of several users transmitting over the same channel, pulses originating in other transmission links may collide with pulses belonging to a reference transmission, giving rise to an interference noise called Multi-user interference (MUI).

**The Isolated Pulse Receiver for Binary Orthogonal PPM**

In binary orthogonal PPM, M = 2 and the two possible transmitted signals are:

$$s_m(t) = \begin{cases} \sqrt{E_{TX}}p_0(t) & \text{for } b = 0. \\ \sqrt{E_{TX}}p_1(t) & \text{for } b = 1 \end{cases} \tag{14}$$

where  $p_0(t)$  is the energy-normalized waveform of the basic pulse,  $E_{TX}$  is the transmitted energy per pulse, and  $\epsilon$  is the time shift introduced by PPM. If  $\epsilon$  is larger than pulse duration  $T_M$ , the set of orthonormal functions can be formed by  $p_0(t)$  and  $p_1(t)$ , that is:

$$s_m(t) = s_{m0}p_0(t) + s_{m1}p_1(t) \quad m=0,1$$

$$\text{where } \begin{cases} s_{00} = \sqrt{E_{TX}} \\ s_{01} = 0 \\ s_{10} = 0 \\ s_{11} = \sqrt{E_{TX}} \end{cases} \tag{15}$$

The optimum receiver scheme for the above signal format is formed by a bank of two correlators,

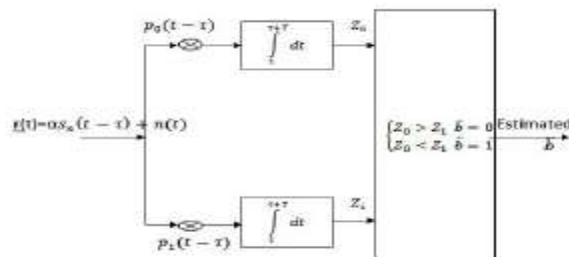


Figure 6: Optimum receiver for 2PPM.



**The Isolated Pulse Receiver for Orthogonal M-ary PPM**

The case of M-ary PPM can be considered an extension of binary PPM. The  $\epsilon$  value is assumed to be larger than pulse duration  $T_M$ . The structure of optimum receiver is shown in fig (4.5), and the decision variables at the output of the signal correlator are

$$\left\{ \begin{aligned} Z_0 &= \alpha s_{m0} + n_0 \\ &\vdots \\ &\vdots \\ &\vdots \\ Z_{M-1} &= \alpha s_{m(M-1)} + n_{M-1} \end{aligned} \right. \quad (16)$$

Where  $s_{mk} = \sqrt{E_{TX}} \int_0^{T_M} p_0(t - m\epsilon) p_0(t - k\epsilon) dt$

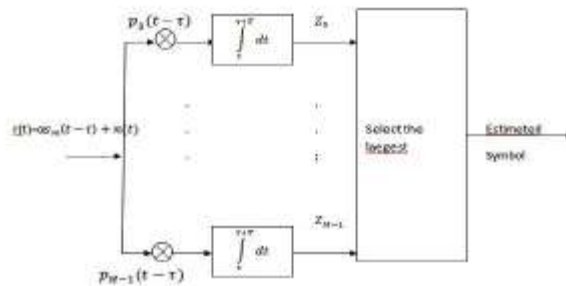


Figure 7: Optimum receiver for M-PPM.

**Simulation Parameters**

The parameters used to evaluate the performance of DS-PPM and PAM .

Table 4.1 Simulation Parameters

Specification	Values
Sampling frequency	50e9
Number of bits	10000
Number of pulses	10000
Gamma	2
distance	10m

**SIMULATION RESULT**

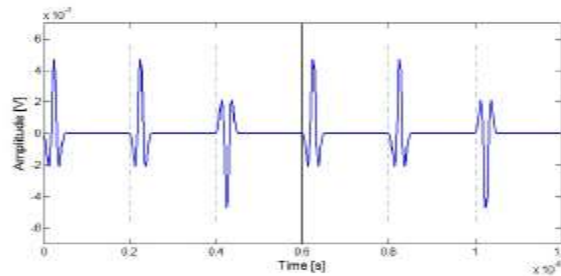


Figure 8: Envelope of received signal

Above Figure shows the envelop of received PPM signal after 10 meters propagation over the

free space.

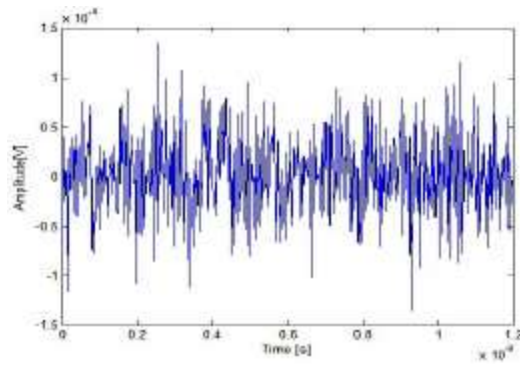


Figure 9: Received Signal rx

Above Figure shows that the effect of noise ( $E_b/N_0 = 0\text{dB}$ ) on the received signal.

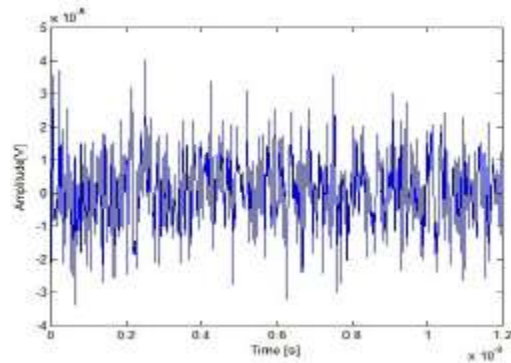


Figure 10: Effect of noise ( $E_b/N_0 = 10\text{dB}$ ) at receiver

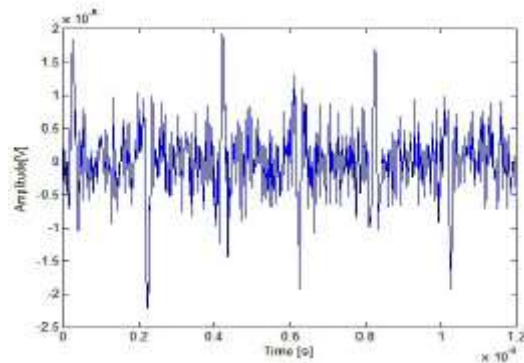


Figure 11: Effect of noise ( $E_b/N_0 = 15\text{dB}$ ) at receiver.

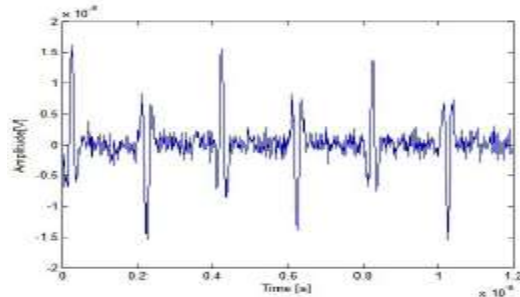


Figure 12: Effect of noise ( $E_b/N_0 = 20\text{dB}$ ) at receiver



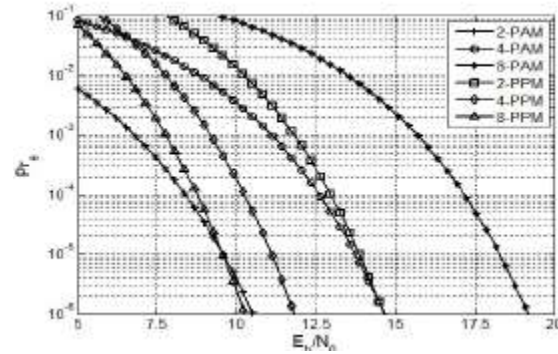


Figure 13: probability of symbol error for M-ary PAM and PPM.

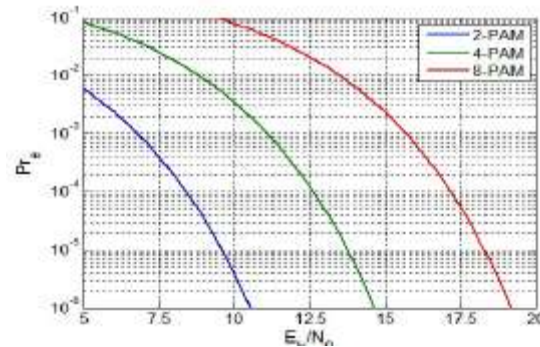


Figure 14: Probability of error for M-ary PAM.

## CONCLUSION

We have calculated the distance between transmitter-receiver and data rate for DS-PAM and DS-PPM system, and in chapter 4 we have calculated the probability of error for DS-PAM and DS-PPM system. It is shown that result obtained using multipath free AWGN channel.

Our comparison results of the presence of Direct-Sequence UWB system for the multipath free AWGN channel, as measured by the probability of error, shows that PAM systems outperforms the PPM systems for all values of SNR. In addition our simulation results show that the system using fifth order pulse performance better than the lower order pulse used system. so pulse selection in UWB is important from the probability of error point of view. UWB systems have been targeted at very High data rate applications over short distances, as well as very Low data rate applications over longer distances. Impulse radio based systems has the ability to trade data rate for link distances. UWB technology is well suited to sensor network applications, with its unique properties of low complexity, low cost, and low power consumption. Moreover, due to the fine time. The low-rate transmission, combined with accurate location tracking capabilities.

## REFERENCES

1. F. Javier Lopez-Martinez, Eduardo Martos-Naya, Jose F. Paris, and Unai Fernandez-Plazaola, "Higher Order Statistics of Sampled Fading Channels With Applications", IEEE Transactions on Vehicular Technology, vol. 61, pp.3342-3346, issue 7, September 2012.
2. Theodore S. Rappaport, Wireless Communications-Principles and Practice, 2ndEd. Prentice Hall, 2000
3. JIA Xiangdong, YANG Longxiang, ZHU Hongbo, "Average Level Crossing Rate and Fading Duration of Multiuser Single Relay Cooperation Wireless Uplinks", IEEE communication, china, vol.10, issue 4, pp.135-143, 2013.
4. Xiangdong Jia, Hongbo Zhu, Longxiang Yang, Second-order statistics of multiuser relay cooperation systems over Nakagami-m fading channels, International Journal of Communication Systems, Wiley, 2013.
5. Khairi Ashour Hamdi, "Analysis of OFDM over Nakagami-m Fading with Nonuniform Phase Distributions", IEEE Transactions on Wireless Communication, vol. 11, pp.488-492 no. 2, February 2012.

6. Yubo Li, Student, Qinye Yin, Li Sun, , Hongyang Chen, and Hui-Ming Wang, "A Channel Quality Metric in Opportunistic Selection With Outdated CSI Over 51BIBLIOGRAPHY Nakagami-m Fading Channels", IEEE Transactions on Vehicular Technology, vol. 61,issue 3,pp.1427-1432, March 2012.
7. Natalia Y. Ermolova and Olav Tirkkonen, "Multivariate  $\chi^2$  -  $\mu$  Fading Distribution with Constant Correlation Model", Communication letters,IEEE,vol.16,issue 4,pp.454-457,2012.
8. Guilherme Silveira Rabelo, Michel Daoud Yacoub and Rausley Adriano Amaral de Souza, "On the Multivariate  $\chi^2$  -  $\mu$  Distribution: New Exact Analytical Formulations", IEEE Transactions on Vehicular Technology vol. 60,pp.4063-4070,no.8 ,October 2011.
9. Norman C. Beaulieu and Kasun T. Hemachandra, "Novel Simple Representations for Gaussian Class Multivariate Distributions with Generalized Correlation", IEEE Transactions on Information Theory,vol 57,no.12,pp.8072-8083,2011.
10. Norman C. Beaulieu and Kasun T. Hemachandra, "Novel Representations for the Bivariate Rician Distribution", IEEE Communications Society,vol.59,issue 11,pp.2951-2954, 2011.
11. Ying Yang, Xiaohui Chen, Wenxiang Dong, Weidong Wang,A general approach to generate Rayleigh fading simulators with correct statistical properties, Wireless Communications and Mobile Computing,Wiley,2011.
12. F. Ramos-Alarcon, V. Kontorovich and M. Lara, "Outage Probability in Nakagami Channels Using Fade Duration Distribution Approximate Results", IEEE Transactions on Communications,vol.58,no.4,pp.1009-1013,April 2010.
13. Daniel Benevides da Costa, JoseCandido Silveira Santos FilhoMiche, Daoud Yacoub and Gustavo Fraidenraich, "Second-Order Statistics of  $\chi^2$ - $\mu$  Fading 52 BIBLIOGRAPHY Channels: Theory and Applications",IEEE communication letters,vol.7,pp.819- 824,March 2008.
14. R. A. A. de Souza and M. D. Yacoub, "Bivariate Nakagami-m distribution with arbitrary correlation and fading parameters", IEEE Transactions Wireless Communication. vol. 7, pp. 5227-5232, Dec. 2008
15. Michel Daoud Yacoub,"The  $\chi^2$  -  $\mu$  Distribution: A Physical Fading Model for the Stacy Distribution", IEEE Transactions on Vehicular Technology,vol.56,no.1,pp.27-34,Jan 2007
16. Lin Yang and Mohamed-Slim Alouini, "Level Crossing Rate over Multiple Independent Random Processes: An Extension of the Applicability of the Rice Formula", IEEE Transactions on Wireless Communications,Vol.6,Issue 12, 2007.
17. Hana Popovic, Dimitrije Stefanovic, Aleksandra Mitic, Ivan Stefanovic, Dusan Stefanovic, "Some Statistical Characteristics of Nakagami-m Distribution",TELSIKS IEEE,pp.509-512,Sep 2007.
18. Da Costa, D.B., Filho, J.C.S.S., Yacoub, M.D., Fraidenraich, G., "Crossing rates and fade durations for diversity-combining schemes over  $\chi^2$  -  $\mu$  fading channels", IEEE Transactions on Wireless Communications,vol. 6, issue 12,pp.4263-4267,Dec 2007.
19. Neji Youssef, Member, Cheng-Xiang Wang, and Matthias Patzold, "A Study on the Second Order Statistics of Nakagami-Hoyt Mobile Fading Channels", IEEE Transactions on Vehicular Technology,vol 54,issue 4,pp.1259-1265,Jul 2005.
20. Gustavo Fraidenraich, Michel D. Yacoub, and Jose Candido S. Santos Filho, "Second-Order Statistics of Maximal-Ratio and Equal-Gain Combining in Weibull Fading", IEEE Communication Letters,vol.9,issue 6, pp.499-501,Jun 2005.
21. Norman C. Beaulieu, Fellow and Xiaofei Dong, "Level Crossing Rate and Average Fade Duration of MRC and EGC Diversity in Ricean Fading", IEEE Transactions Communication,vol 51,issue 5,May 2003.
22. Cyril-Daniel Iskander and P. Takis Mathiopoulos, "Analytical Level Crossing Rates and Average Fade Durations for Diversity Techniques in Nakagami Fading Channels", IEEE Transactions on Communications,vol.50,no.8,pp.1301-1309,Aug 2002.
23. Abdi A., Kaveh Mostafa, "Level crossing rate in terms of the characteristic function a new approach for calculating the fading rate in diversity systems", IEEE Transactions on Communication, vol. 50, no. 9, 2002.